Visual Cortex Responses to Single- and Simultaneous Multiple-Electrode Stimulation of the Retina: Implications for Retinal Prostheses

Mohit N. Shivdasani,[1] *James B. Fallon,*[1] *Chi D. Luu,*[2] *Rosemary Cicione,*[1] *Penny J. Allen,*[2] *John W. Morley,*[3] *and Chris E. Williams*[1]

Purpose. The aim of this study was to compare simultaneous stimulation of multiple electrodes to single-electrode stimulation in a retinal prosthesis.

Methods. A platinum electrode array was implanted into the suprachoroidal space in six normally sighted anesthetized cats. Multiunit activity from the primary visual cortex in response to retinal stimulation was recorded. Cortical thresholds, yield of responses, dynamic ranges, and the spread of retinal activation were measured for three modes of stimulation: single electrode, half-row (six-electrode horizontal line), and column (seven-electrode vertical line).

Results. Stimulation of the best half-rows and columns was found to elicit activity with higher yield and lower charge thresholds per electrode compared to the best single electrodes. Dynamic ranges between the three modes were similar. As expected, peak voltages measured for columns and half-rows were lower than those measured for single electrodes. Spread of retinal activation, determined by the increase in threshold with distance in the retina from the best site, was found to be similar between single- and multiple-electrode stimulation but dependent on orientation.

Conclusions. The lower thresholds, higher yield, equivalent dynamic ranges, and equivalent spread of retinal activation observed from simultaneous stimulation of multiple electrodes may be due to current and/or neural summation within the retina. Such stimulation techniques could be useful for the presentation of lines and edges of objects using a suprachoroidal retinal stimulator with low voltage compliance. Furthermore, the results suggest that more complex visual processing strategies in addition to sequential stimulation of individual electrodes should be considered for retinal prostheses. (*Invest Ophthalmol Vis Sci.* 2012;53:6291–6300) DOI:10.1167/iovs.12-9434

In recent years retinal prostheses have gained a lot of interest for the treatment of degenerative disorders such as retinitis pigmentosa. The prosthesis aims to restore some vision by electrically stimulating the surviving neurons within the retina via an electrode array that is either directly placed on the inner surface of the retina (epiretinal), between the retinal pigment epithelium and inner nuclear layers (subretinal), between the sclera and the choroid (suprachoroidal), or penetrating through the sclera (transscleral). There are at least six different groups worldwide that have conducted both acute and chronic human clinical trials with electrode arrays implanted in different retinal locations.[1–9] These trials have highlighted that electrical stimulation of the retina is safe; most individual electrodes on the array are effective in generating discrete perceivable phosphenes; and most patients can perform basic navigation and object discrimination tasks, while some can perform complex tasks such as reading letters and simple words in a controlled environment. Despite these promising outcomes, there is significant variability in performance among patients and research groups. Some patients report phosphene perception on only few electrodes, while for others phosphene vision is nowhere near the level required for independent mobility.[10–13] It is believed that increasing the number of electrodes that are capable of generating discriminable phosphenes should achieve a higher resolution and therefore provide improved performance; however, this approach comes with its own engineering and safety challenges that must be overcome.[10–13]

An alternative approach to achieving higher performance with a retinal prosthesis may be to improve the stimulation strategy algorithms responsible for decoding and representing incoming visual information in the form of electrical pulses. In most externally powered prosthesis designs, these algorithms are normally stored within an external vision processor that receives visual information from a camera. However, less is known about the stimulation strategies employed within the various retinal prostheses currently in human trial. Indeed, it is still unclear as to how best to make use of the primitive phosphenes seen with electrical stimulation of individual electrodes to ultimately construct an image to provide meaningful vision. It is reasonable to assume that, in its simplest form, each frame recorded by the camera would be represented as a two-dimensional grid of discrete "pixels," then each pixel allocated to an individual electrode on the array. The implementation of such a strategy could then be achieved by sequential stimulation of individual electrodes at frequencies equal to or beyond that of flicker fusion (~40–50

From the [1]Bionics Institute, East Melbourne, Victoria, Australia; the [2]Centre for Eye Research, University of Melbourne, Royal Victorian Eye & Ear Hospital, East Melbourne, Victoria, Australia; and the [3]School of Medicine, University of Western Sydney, New South Wales, Australia.

Supported by the Australian Research Council through its Special Research Initiative in Bionic Vision Science and Technology awarded to Bionic Vision Australia and the Bertalli Family Foundation to the Bionics Institute. Additional support is received from the Victorian Government through its Operational Infrastructure Program. CERA receives Operational Infrastructure Support from the Victorian Government.

Submitted for publication January 4, 2012; revised April 25 and August 14, 2012; accepted August 14, 2012.

Disclosure: **M.N. Shivdasani**, P; **J.B. Fallon**, None; **C.D. Luu**, None; **R. Cicione**, None; **P.J. Allen**, None; **J.W. Morley**, None; **C.E. Williams**, P

Corresponding author: Mohit N. Shivdasani, Bionics Institute, 384-388 Albert Street, East Melbourne, Victoria 3002, Australia; mshivdasani@bionicsinstitute.org.

Hz[14]) and the frame rate of the camera. However, as the number of electrodes on the array in future devices are planned to be increased to a few hundreds or even into the thousands to provide higher resolution, the method of sequential stimulation may not be viable as each electrode may require a finite amount of stimulation time (usually ranging between 200–1000 μs[4,8]) to produce a reliable phosphene within safe limits of charge and voltage compliance limits of the stimulator. To overcome this limitation, simultaneous stimulation of multiple electrodes could be an alternative approach to ensure full coverage of the electrode array. In cochlear implants, simultaneous stimulation of two or more electrodes has been found to produce significant channel interaction.[15–17] Because channel interaction is unpredictable, often resulting in undesirable perceptual effects, current pulses in cochlear implants are typically delivered sequentially to a single electrode at a time.[18] However, if the induced electric field by applying current on each electrode is localized enough, then in theory several electrodes could be stimulated simultaneously without much "cross-talk."[19] For example, using a hexagonal guard return around each stimulated electrode as proposed by Dommel et al.[20] may alleviate some of the issues with channel interactions and allow simultaneous stimulation of multiple electrodes.

Initial human trials of both sequential[2,4,14] and simultaneous[2,21–23] stimulation of contiguous electrodes, albeit not limited to just retinal stimulation but also stimulation of the visual cortex,[23] have proven that patients can discriminate simple patterns such as horizontal and vertical lines or even simple letters. More recently, Wilke et al.[2] showed that patients with a 16-electrode subretinal array could discriminate between different orientations of lines represented by simultaneous stimulation of contiguous electrodes that formed a line and could recognize simple letters made up from sequential stimulation of single electrodes. They also found that one patient could discriminate sequential stimulation of two parallel lines.[2] These results are encouraging in that they confirm that simultaneous stimulation of multiple electrodes in the retina can produce meaningful percepts in blind humans. When it comes to implementation in a stimulation strategy, there are two ways in which simultaneous stimulation of multiple electrodes can be achieved: either employ "parallel" stimulation using multiple sources as performed by the Second Sight group in the retina[21,22] and by Brindley and Lewin in the visual cortex,[23] or "gang" groups of electrodes together and connect them to a single source as performed by Wilke et al.,[2] with each method having its own merits. For example, parallel stimulation would enable precise control of the charge delivered through each individual electrode owing to the use of multiple current sources and could thus be used to tune perceptual characteristics of the line or pattern being formed. In contrast, the advantage of ganged stimulation with a single current source would be the overall lower electrode impedance "seen" by the stimulator and therefore lower excursion voltages on the electrodes. Perhaps more intriguing than the lower impedances is the reduction in thresholds (on a per electrode basis) found with ganged stimulation, reported previously by our group in normally sighted cats with suprachoroidal stimulation[24] and by the Retina Implant AG group in blind humans with subretinal stimulation (Wilke R, et al. *IOVS* 2010;51:ARVO E-Abstract 2026).

In light of recent results,[2] it is important to further study and understand how the visual cortex responds to ganged stimulation of multiple electrodes in the retina and ascertain whether there are any differences in responses to single-electrode stimulation. Results from these experiments may provide insights into developing stimulation strategies that can take advantage of simultaneous multiple-electrode stimulation with the aim of providing meaningful percepts that will appropriately represent objects within an image. As a first step toward this, we undertook a series of experiments recording multiunit spike activity across the visual cortex in response to single and ganged electrode stimulation of the retina via an electrode array placed in the suprachoroidal space of anesthetized cats. The results from this study have provided data on the relative benefits of simultaneous multiple-electrode stimulation as opposed to single-electrode stimulation.

Materials and Methods

Anesthesia and Surgery

Protocols used for anesthesia and surgery are described in detail in a previous study performed by our group.[24] All procedures were approved by the Royal Victorian Eye and Ear hospital animal ethics committee and complied with the ARVO statement for use of animals in ophthalmic research. Normally sighted adult cats ($n = 6$) were anesthetized with ketamine (intramuscular [IM], 20 mg/kg) and xylazine (subcutaneous [SC], 2 mg/kg), followed by intravenous infusion of sodium pentobarbitone (60 mg/mL, 1:6 dilution). Animals were treated with dexamethasone (IM, 0.1 mg/kg) and clavulox (SC, 10 mg/kg) at regular intervals as well as a continuous intravenous infusion of Hartmann's solution (sodium lactate, 1.5 mg/mL/hour). Anesthetic flow rate was adjusted based on continuous monitoring of respiration rate, end-tidal CO_2, and core body temperature (37°C). A lateral canthotomy followed by a full-thickness incision through the sclera was performed to expose the choroid. A "pocket" was made within the suprachoroidal space, and a flexible electrode array (details below) was inserted 15 to 17 mm into each eye (total of 12 eyes). Effort was made to place the tip of the array beneath the area centralis. Once the position was finalized, the array was sutured to the sclera for stability.[25] A platinum ball electrode (1.5-mm diameter) was implanted into the vitreous humor as a return electrode for monopolar stimulation. Following implantation, the animal was placed in a stereotaxic frame (David Kopf Instruments, Tujunga, CA). Clinical assessment of the eye and taking of a fundus photograph was performed, following which a craniotomy was performed to expose the primary visual cortex. Experiments were typically conducted over 3 to 4 days; and, at the end of each experiment, animals were euthanized using an overdose of sodium pentobarbitone (150 mg/kg, intraperitoneal).

Suprachoroidal Electrode Array

The suprachoroidal electrode array (Fig. 1A) was similar in design to the one used in our previous study[24] and manufactured through Flexible Circuit Technologies (Plymouth, MN). It consisted of a flexible polyimide substrate (25 μm thick) with exposed gold electrode sites (400-μm diameter, 0.00126-cm^2 surface area) arranged in a 7 row × 12 column grid with 1-mm pitch between sites (0.8-mm spacing between adjacent rows, 1-mm spacing between adjacent columns). The exposed gold sites were electroplated with platinum (~1 μm thick) to increase their charge injection capacity. Prior to implantation, the electrode array (except connectors and electrode sites) and surrounding edges were coated with medical grade silicone to avoid sharp edges and minimize trauma during insertion (Permatex, CT; Type 65AR flowable; 150–400 μm tapered thickness from tip).

Stimulation and Recording of Retinal Voltage Waveforms

All stimulation and recording protocols were performed in an electrically shielded and darkened Faraday room to avoid electrical noise and retinal illumination effects. Individual electrodes on the retinal array were routed through a custom switching system described by John et al.[26] A 512 cross-point switch array (PXI 2532; National

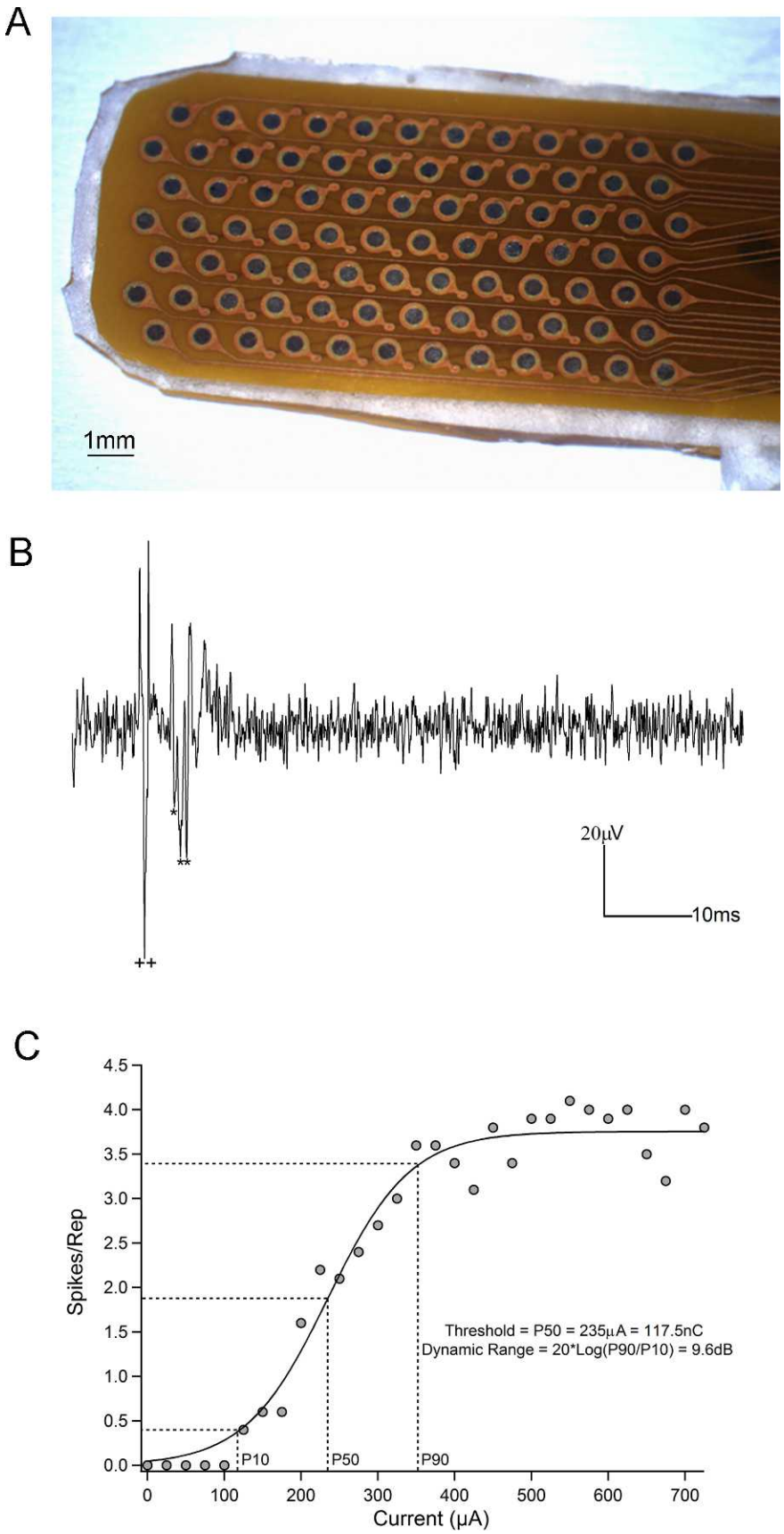

Figure 1. (**A**) Photomicrograph of retinal electrode array with 7 rows × 12 columns of platinum electrodes. (**B**) Typical recording from one cortical channel in response to stimulation of a single electrode. ++ denotes stimulus artifact, while * denotes occurrence of spikes post-stimulus. (**C**) Typical input–output function from one cortical channel. Threshold was defined as the current required to elicit 50% of the maximum spike rate (P50), while dynamic range was defined as the ratio of the currents required to elicit 90% (P90) and 10% (P10) of the maximum spike rate, expressed in decibels.

Instruments, Austin, TX) containing electronic reed relays was configured as a 4 × 128 multiplexer and, along with software developed in-house, was used to connect to single electrodes as well as form patterns of multiple ganged electrodes.[26] Using a single cathodic-first, biphasic, charge-balanced pulse (200 μA, 250 μs per phase, 25-μs interphase gap) delivered with an in-house custom-built constant current stimulator, the resulting induced voltage waveform between each active electrode on the retinal array and the monopolar vitreous return was recorded (example of current and voltage waveforms shown in Fig. 2A). During the interphase gap, the stimulator was kept open circuited; and, at the end of the second phase, the active and return electrodes were shorted. Using the voltage waveforms, the peak voltage at the end of the cathodic (first) phase was measured. In addition to single electrodes, voltage waveforms were also recorded with multiple electrodes ganged together either in a half-row (first six contiguous electrodes from the tip forming a horizontal line) or column (seven contiguous electrodes forming a vertical line). Peak cathodic electrode voltages for columns and half-rows were compared to those for single-electrode stimulation (Fig. 2B).

Stimulation and Cortical Recordings

For initial cortical recordings, a platinum ball electrode was placed on the extradural surface of the visual cortex close to the posterior lateral gyrus, corresponding to the area centralis region of the retina[27] along with a platinum needle reference electrode implanted in a skinfold at the back of the neck. Evoked potentials were recorded with this electrode in both cortical hemispheres every 0.5 to 1 mm along the caudo-rostral dimension in response to stimulation of a column of retinal electrodes (typically column 3) versus the monopolar return, using cathodic-first, biphasic, charge-balanced current pulses (0–5 mA, 500 μs per phase, 25-μs interphase gap). The cortical area with the lowest evoked potential threshold to electrical stimulation was chosen to implant a multichannel recording array following removal of the dura mater above the chosen location. Typically, implantation of the recording array occurred in the hemisphere contralateral to the eye used for electrical stimulation and in the cortical area that corresponded reasonably well with the location of the tip of the retinal array in the visual space, based on the fundus image.[27] The recording arrays used were either a 32-channel (four shanks with 400-μm separation × eight electrodes with 200-μm separation) silicon substrate array (NeuroNexus Technologies, Ann Arbor, MI) or a 49- (7 × 7) or a 60-channel (6 × 10) "Blackrock" array (400-μm electrode separation; Blackrock Microsystems, Foxborough, MA). The Neuronexus array sampled approximately 1.2 mm of cortical space in the caudo-rostral direction[27] and was inserted to an average depth of 2.5 mm below the dorsal surface of V1. In comparison, the Blackrock arrays sampled a larger area (2–2.4 mm medio-lateral direction, 2.4–3.6 mm caudo-rostral direction) of cortical space[27] and penetrated the cortex to a depth of approximately 1 mm.

Multiunit activity (0.3 Hz–7.5 kHz bandpass filtered, 30-kHz sampling rate) was recorded in response to monopolar electrical stimulation of single electrodes, half-rows, and columns on the suprachoroidal array using the Cerebus recording system (Blackrock Microsystems, Salt Lake City, UT). In one experiment, other configurations of six or seven contiguous ganged electrodes that did not form a line were tested and compared to single electrodes. Pulse width and interphase gap were fixed at 500 μs per phase and 25 μs, respectively. Current varied randomly from zero to 725 μA for single electrodes (25-μA steps), zero to 4.4 mA for half-rows (200-μA steps), or zero to 5 mA for columns, (200-μA steps). Each current level was repeated 10 times. The maximum currents ensured that charge densities were kept below 300 μC cm^{-2}.

Data Analysis

Data analysis for each cortical recording site was performed offline using custom scripts in Igor Pro (Wavemetrics, Lake Oswego, OR). Signal artifacts were first removed using similar techniques as described by Heffer and Fallon.[28] An estimate of the background activity was made by calculating the root mean square (RMS) value of the incoming signal in a moving 60-second window. Multiunit spikes (bandpass filtered, 0.3–5 kHz) were detected (Fig. 1B) and time-stamped when the signal was found to exceed 4.2 times the RMS value. Spike rates were analyzed in the first 3 to 20 ms from stimulus onset at each current level to obtain a spike-rate versus current-level input–output function (Fig. 1C) for each of the stimulated single electrodes, half-rows, and columns in the retina. A sigmoid curve was fitted to each input–output function, from which thresholds and dynamic ranges were determined. Threshold was defined as the current required to elicit a spike rate equal to 50% of the maximum saturating spike rate, expressed as charge (in nC, Fig. 1C). Dynamic range was defined as the ratio of the currents required to elicit spike rates equal to 90% and 10% of the maximum saturating spike rate, expressed in dB (Fig. 1C).

Given the well-defined mapping of neurons between the retina and the visual cortex[27] and the known nature of receptive fields of cortical neurons in the cat,[29,30] we expected that for each cortical recording site there would be a "best" single electrode, half-row, and column on the retinal array or in other words a "hot spot" that would evoke activity with a lower threshold compared to any other single electrodes, half-rows, and columns. These lowest threshold sites in the retina were termed the best single electrodes, best half-rows, and best columns (collectively referred to herein as best lines), and their respective thresholds were collectively termed as the best thresholds. Correspondingly, the dynamic ranges from each of the best electrodes, half-rows, and columns were termed as the best dynamic ranges. Best thresholds and best dynamic ranges were then compared between single electrodes and lines in the retina across all cortical recording sites using a one-way repeated measures ANOVA (Sigmaplot v. 12; Systat Software, San Jose, CA). In addition to estimating thresholds and dynamic ranges, we determined the degree of the spread of retinal activation for each cortical recording site. This was performed by calculating the increase in threshold of every retinal single electrode and line from the threshold of the best electrode or line for each recording site. The increase in threshold was expressed as a decibel change and plotted as a function of the distance in the retina from the best electrode or line. Differences in the degree of the spread of retinal activation were compared between single electrodes and lines for all cortical recording sites using a two-way repeated measures ANOVA with stimulation mode (three levels: single, half-row, and column) and distance from the best site in the retina (three levels: 0.8–1.6 mm, 1.6–2.4 mm, and 2.4–3.2 mm) as the two within-subject factors. All values reported are mean ± standard error of mean.

Results

Due to surgical complications, data was collected and analyzed from stimulation of only nine eyes. Also, due to time constraints and the large number of electrodes on the retinal array, it was not possible to electrically stimulate all single electrodes, half-rows, and columns in every experiment. In nine eyes of six animals, 261/756 single electrodes, 63/63 half-rows, and 87/108 columns on the retinal array were stimulated. A total of 339 cortical recording sites from six animals were analyzed for responses. A given cortical site was deemed responsive if it exhibited a threshold to stimulation of a single electrode, half-row, or column in the retina. Not all stimulation sites in the retina were found to evoke a cortical response. Of the total number of retinal electrodes stimulated, 39.5% of single electrodes, 82.6% of half-rows, and 57.5% of columns elicited a response on at least one cortical site. Mean first spike latency at the maximum current presented on all stimulating electrodes from all cortical sites was found to be 6.96 ± 0.03 ms.

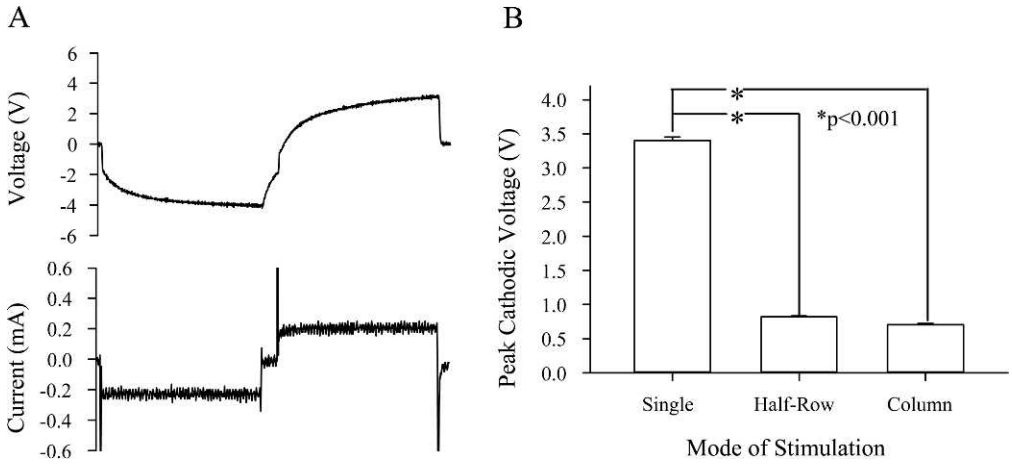

Figure 2. (**A**) Typical voltage and current waveform recorded in vivo from stimulation of a single electrode on the suprachoroidal array (200 μA, 250 μs). (**B**) Peak cathodic voltages measured with single electrodes, half-rows, and columns from all experiments. Voltage excursions measured for lines were found to be significantly lower than those measured for single electrodes.

Figure 2A shows a typical current and resultant voltage waveform for a single electrode. Peak cathodic voltages recorded in the retina from single electrodes ($n = 420$), half-rows ($n = 35$), and columns ($n = 60$) are shown in Figure 2B. A one-way ANOVA revealed that peak cathodic voltages measured using half-rows and columns did not significantly differ from each other and there was an approximate 4- to 5-fold decrease ($P < 0.001$) in peak cathodic voltage when stimulating lines were compared to single electrodes using the same current amplitude.

Of the total of 339 cortical sites analyzed, only sites for which a best single electrode, best half-row, and best column could be found were chosen for further analyses ($n = 219$). Using the fundus images taken after surgery, which clearly showed the outline of the position of the array in the suprachoroidal space, we estimated the approximate positions of the best single electrodes for all 219 cortical sites and overlaid them on the fundus images in all six animals (Fig. 3). Best single electrodes were found to mostly be located near the area centralis, which in most animals was where the tip of the array was placed. The columns that were closer to the tip of the electrode array (columns 1–3) were found to make up the majority of the best columns (data not shown), while best half-rows tended to belong mostly to the central spine of the electrode array (row 4) or were located closer to the edges of the electrode array (rows 1, 2, and 6), depending on the orientation of the tip and whether it was a left or right eye implantation (data not shown). In addition, best single electrodes were found to be mostly located at the intersection of the best columns and best half-rows. These results were consistent with both the position of the tip of the retinal electrode array and the position of the cortical recording array being aligned with the area centralis.

Figure 4A shows best thresholds from 219 cortical sites (calculated as charge in nC) for the three modes of stimulation. Overall, best columns and half-rows required more total charge to achieve threshold at a given cortical site compared to best single electrodes. However, when thresholds were calculated as charge per electrode (total charge divided by the number of electrodes ganged together), lines were found to have significantly lower thresholds compared to single electrodes by at least 50% (Fig. 4B, one-way repeated measures ANOVA, $P < 0.001$). Among the two line orientations, half-rows elicited cortical responses with lower thresholds per electrode compared to columns; however, this was borderline significant ($P = 0.046$). Similar results were obtained when comparing cortical thresholds from simultaneous stimulation of groups of contiguous electrodes not forming a line to single-electrode stimulation, in that the threshold charges required per electrode for six or seven contiguous ganged electrodes were significantly lower than those for single electrodes. In contrast, despite cortical best thresholds being dependent on the mode of stimulation, best dynamic ranges (Fig. 4C) were not found to be significantly different between single electrodes and lines. Dynamic ranges were typically found to be in the range 1 to 15 dB but could extend up to more than 25 dB for some cortical sites.

A final outcome that we assessed was the degree of localization of cortical activity from stimulation of single electrodes and lines. Figure 5 depicts representative cortical image spike profiles recorded with a Blackrock array from stimulation of a single electrode, half-row, and a column in one experiment. Single-electrode stimulation mainly evoked a punctate spot-like area of cortical activation (reminiscent of a phosphene). Stimulation of half-rows and columns was found to evoke more diffuse cortical activation that resulted in "lines" of cortical activity. Interestingly, changing the orientation in the retina from a half-row to a column was found to change the orientation of the line of cortical activity (Fig. 5). Further, stimulation of columns in the retina was found to induce more spiking activity along the caudo-rostral dimension of the cortex; whereas, with half-rows, activation was spread along the medio-lateral dimension. Given our experimental protocols, it is likely that stimulation of columns would have activated areas parallel to the vertical meridian in the retina, while stimulation of half-rows would more likely activate areas parallel to the horizontal meridian. Therefore, it was encouraging to observe that activation profile shapes in the cortex were not only generally consistent with the patterns of stimulation performed in the retina, but also exhibited a degree of retinotopicity.[27] It was difficult to quantify the degree of localization of cortical activity for each and every stimulated single electrode, half-row, and column for two main reasons. First, we did not use the Blackrock array for recordings in all experiments; therefore, experiments in which only a penetrating "Neuronexus" array was used did not cover sufficient area across the surface of the visual cortex to be able to observe the full "two-dimensional" extent of activation. Second, even in the experiments where a Blackrock array was used for recording, the positioning of the recording array had to be well aligned with the position of the retinal array to cover enough of retinal/visual space in order to be able to observe

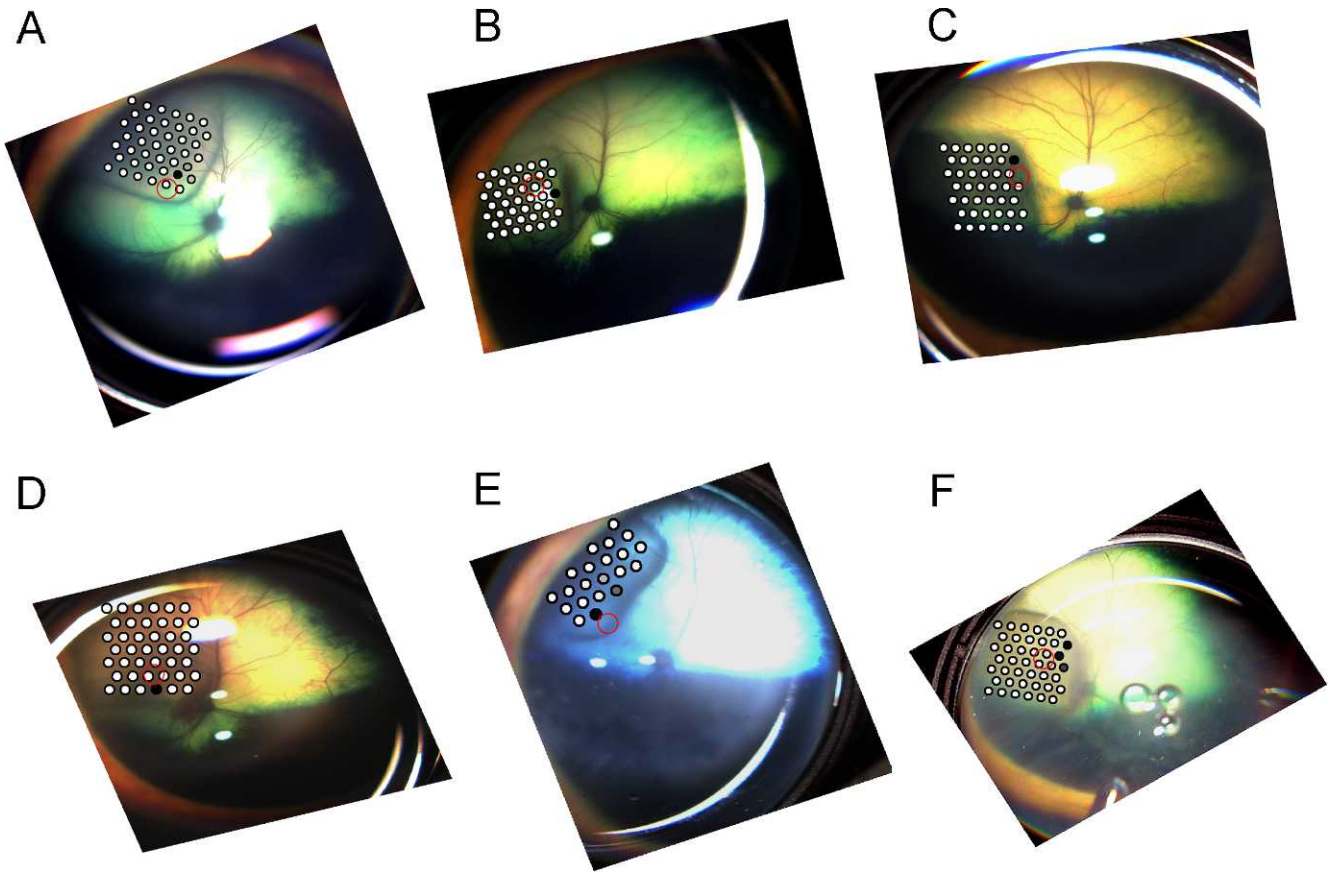

Figure 3. (**A–F**) Fundus images from six experiments, showing position of retinal array in the suprachoroidal space. Overlaid are the approximate positions of individual electrodes on each array. *Red circles* on each fundus image indicate approximate location of area centralis. In each experiment, for all cortical sites the number of times a particular single electrode was chosen as the best electrode is indicated from minimum (*white*) to maximum (*black*). All images have been appropriately oriented with superior retina shown toward the top and temporal retina to the left.

the full extent of cortical activation. As a result, cortical activation profiles that were consistent with the pattern of electrical stimulation employed were observed in approximately half of the recording arrays where a Blackrock array was used.

As an alternative to quantifying the degree of localization in the cortex, we quantified the degree of spread of activation in the retina. We were able to perform this analysis on individual cortical electrodes on both the Neuronexus and Blackrock arrays ($n = 92$). For each cortical site, we used the increase in threshold with every millimeter shift across the retina from the best stimulation site as an indication of retinal spread of activation. Figure 6 shows the retinal spread of activation as a function of distance from the best site in the retina. For a shift of one single electrode or one half-row or one column in the retina from the best electrode or the line, cortical thresholds on average increased by 3 to 5 dB. Thresholds were found to further increase with larger shifts in the retina, with up to 8 to 12 dB increase in threshold from the best threshold at retinal sites that were three or more millimeters away from the best sites. A two-way repeated measures ANOVA revealed that the degree of spread of retinal activation was similar when comparing single electrodes against half-rows and columns ($P > 0.05$); however, half-rows were found to have a small but significantly higher degree of retinal spread of activation compared to columns ($P < 0.05$). No significant interactions were found between mode of stimulation and distance ($P > 0.05$).

Discussion

The main focus of this study was to systematically assess if multiple-electrode stimulation in the form of a line of contiguous electrodes using a single current source offered benefits over single-electrode stimulation. A priori, it would be expected that multiple-electrode stimulation would offer an advantage in terms of lower electrode excursion voltages. We also found that multiple-electrode stimulation exhibited a higher yield of cortical responses compared to single-electrode stimulation. On reflection, this result was expected given that stimulation of lines resulted in activation of a fairly wide area across the retina (~5–6 mm of retinal space corresponding to ~20–24° of visual space[30]), thereby increasing the likelihood of producing a response on a given cortical site. Despite the use of normally sighted cats and suprachoroidal stimulation, the mean first spike latency in our study was consistent with other studies measuring cortical multiunit activity in response to both subretinal and epiretinal stimulation.[31,32] Furthermore, the latencies from the present study were also consistent with the electrically evoked latencies found in a previous study by our group and were substantially shorter than the visually evoked latencies found in that study.[24] This suggests that the responses seen in the present study were not as a result of photoreceptor activation but more likely a result of direct activation of ganglion cells. Further experiments using appropriate synaptic blockers in normally sighted animals or using animals with retinal degeneration are required to assess

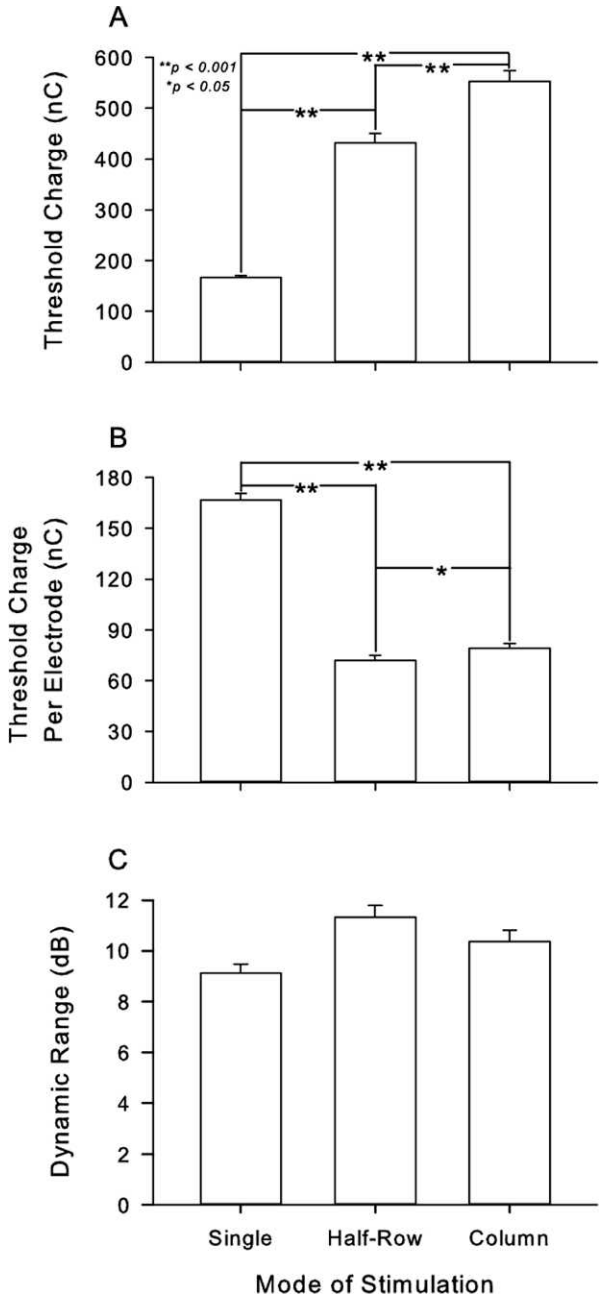

Figure 4. (**A**) Overall thresholds. (**B**) Thresholds as charge per electrode. (**C**) Dynamic ranges for the best single electrodes, best half-rows, and best columns.

which retinal cells form the target for suprachoroidal stimulation. We also found that stimulation of lines elicited spiking activity in the visual cortex, with several-fold reduction in charge thresholds on a per electrode basis, equivalent dynamic ranges, and equivalent spread of activation in the retina compared to single-electrode stimulation. In addition, we found that threshold reductions were not specific to line stimulation but were also possible if multiple electrodes were ganged together as a group of contiguous electrodes. Below we discuss possible mechanisms behind our results and suggest ways of using multiple-electrode stimulation to improve the efficacy of retinal stimulation strategies.

There are two obvious mechanisms that may explain the lower charge per electrode required to reach cortical threshold seen with multiple-electrode stimulation. The most parsimonious explanation is current summation within the retina due to overlapping electric fields. Current summation with simultaneous stimulation of electrodes is a well-known issue with cochlear implants.[15–18] In fact, early "continuous analog" stimulation strategies used in cochlear implants were discontinued because current summation would result in uncontrollable loudness interactions.[33] Current summation has also been explored to some extent with epiretinal stimulation in blind humans.[22,34] In recent studies by the Second Sight retinal implant group examining spatiotemporal interactions with paired or multiple-electrode stimulation,[22,34] it is reported that when stimulating with temporally overlapping pulses (with resultant overlapping electric fields), to match brightness levels, the charge required is significantly lower (by up to 20%) than for temporally nonoverlapping pulses. Furthermore, in a recent modeling study of the retina assessing electric field profiles with simultaneous multiple-electrode stimulation, Wilke et al.[19] report that as the number of concurrently activated electrodes is increased, the penetration depth of the resultant summed electric field is also increased. Therefore, it is possible that current summation as a result of simultaneous stimulation of multiple electrodes in the present study enabled the induced electric fields to better penetrate through the choroid and tapetum layers. This would in turn provide an increased likelihood of sufficient current reaching the retina.

A second possible explanation is the summation of neural activity from retinal areas directly underlying the electrodes. Indeed, in the paired-electrode stimulation study by Horsager et al.[34] using varying phase shifts between paired stimuli, even pulses where electric fields are nonoverlapping in time are seen to induce summation interactions up to phase shifts as long as 9 ms. Also, studies that employ sequential stimulation of individual electrodes for pattern presentation report that patients see a contiguous percept without any gaps between nonoverlapping pulses on electrodes.[2,14] These results strongly suggest that neural spatiotemporal mechanisms of integration may play a role in providing summed information from the retina to the visual cortex. Early and more recent studies that explore receptive fields in the cat visual cortex suggest that some complex cortical cells can have receptive fields that are more than 15° in width[29] and that formation of both simple and complex receptive fields in the cortex arise from a large degree of convergent information coming from the retina and lateral geniculate nucleus of the thalamus.[35] Although stimulation of lines in our study would have resulted in much larger areas than 15° of visual space being stimulated, it is possible that neural summation in part may have resulted in reduced thresholds and high response yield found with multiple-electrode stimulation. Having proposed neural summation as a possibility, though, it is unknown whether this summation would exclusively arise from the retina as it could also arise within the lateral geniculate nucleus or within the primary visual cortex itself. Systematic electrophysiology studies employing multiple current sources and varying degrees of simultaneous and nonsimultaneous stimulation protocols would need to be performed to answer this.

It was important to assess if impedance variations between single electrodes could partly be responsible for lines exhibiting lower charge per electrode thresholds compared to single electrodes. A potential problem with ganging of electrodes is that, due to likely impedance variations between individual electrodes forming a pattern, current distributions among the electrodes will not be equal. In the present study, although electrode impedances were not measured, we were able to use the electrode peak cathodic voltage and current data from single electrodes used to make up the columns and half-rows to reasonably estimate the current distributions that

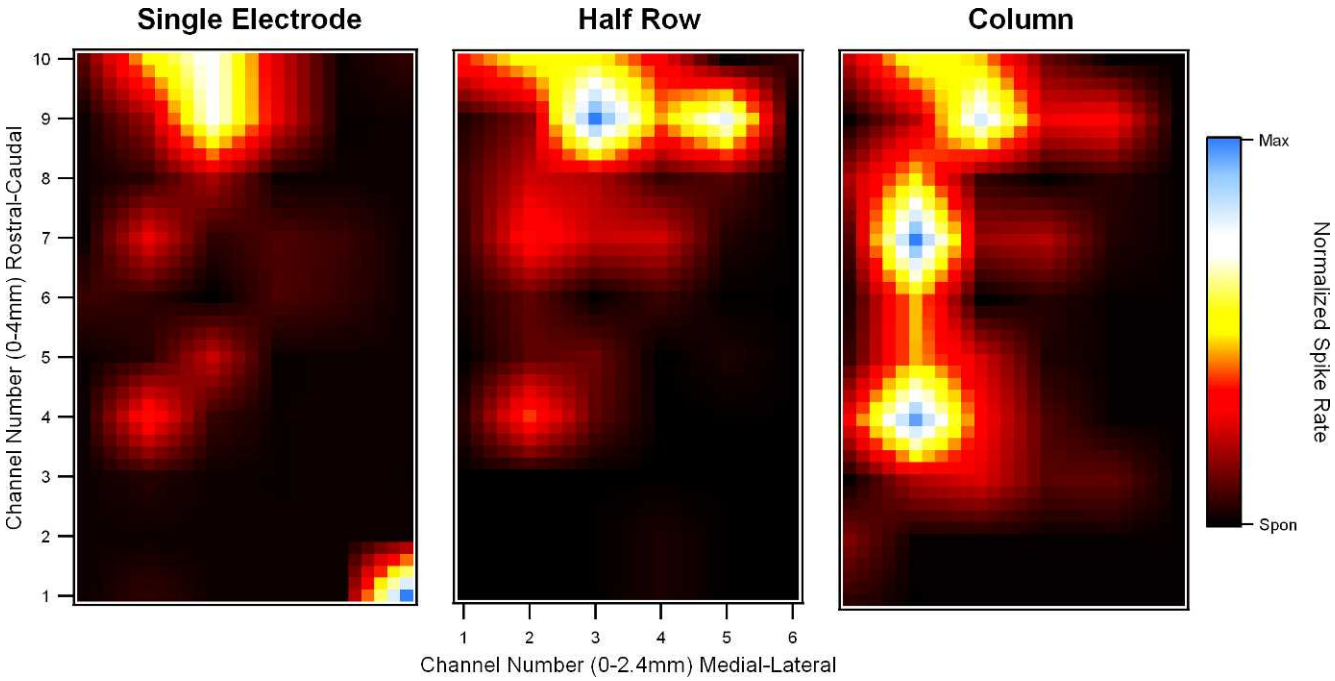

Figure 5. Cortical activation profiles recorded in the primary visual cortex using a 60-channel Blackrock array from electrical stimulation of a single electrode (*left panel*), half-row (*middle panel*), and a column (*bottom panel*) in the retina. Colors indicate normalized spike rates from spontaneous activity (*black*) to maximum activity (*yellow*).

would have occurred during ganged stimulation. These current distributions were compared to the expected current distributions, assuming equal impedance conditions on all single electrodes making up a given column or half-row. Deviations of the actual current distributions from the expected current distributions were calculated for each individual electrode within a column or half-row. We found that, on average, for any given electrode within a column or half-row, the deviation in actual current from the expected current was 2.7% ± 0.1% (maximum 12.1% deviation) for electrodes within columns and 2.6% ± 0.2% (maximum 12% deviation) for those within half-rows. These results indicate that, even though there may have been unequal current distributions during ganged stimulation due to impedance variations between electrodes, these were not significant and therefore not sufficient to explain the threshold benefits seen with ganged stimulation.

We also found that stimulation of lines in our study yielded equivalent dynamic ranges to single-electrode stimulation.

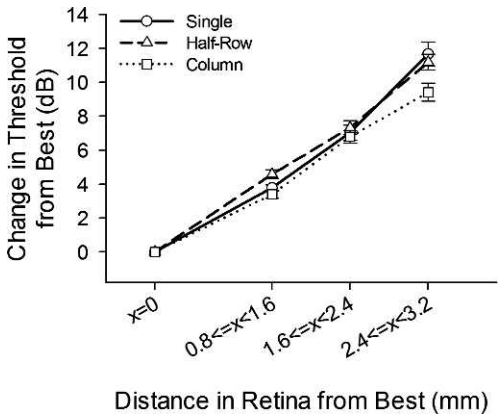

Figure 6. Degree of spread of retinal activation from stimulation of single electrodes versus that from stimulation of lines.

Although dynamic range does not necessarily indicate the degree of brightness resolution that can be achieved through controlling current levels with stimulation, generally a large dynamic range is believed to be beneficial. Nevertheless, our results suggest that if phosphene brightness is controlled by varying current levels, then this can be achieved with stimulation of both single electrodes and lines. Another piece of evidence supporting that current spread from line stimulation was generally confined within the region of the electrodes being stimulated was the similar degree of spread of retinal activation found between lines and single-electrode stimulation. For any given recording site in the cortex, it required approximately 3 to 5 dB more charge to reach threshold per millimeter shift in the retina, regardless if it were a shift in the line or a shift in a single electrode. Thus, both lines and single electrodes resulted in punctate retinal stimulation. It is unclear as to why, between the two orientations of line stimulation used in this study, half-rows performed better than columns in that their thresholds were lower and the degree of spread of retinal activation was higher. Although beyond the scope of the results of this study, a possible explanation is that retinal ganglion cells and cortical neurons were more orientation specific along the horizontal meridian compared to the vertical meridian. While it is well known that orientation sensitivity is a distinctive feature of cortical neurons,[30,36] several studies have also shown that most retinal ganglion cells in cats are sensitive to stimulus orientation and may prefer more horizontally oriented stimuli owing to their dendritic field orientation.[37,38] Another possible scenario, although more relevant to an epiretinal electrode placement rather than a suprachoroidal placement, is that during half-row stimulation, individual retinal ganglion cell axons may have been stimulated at multiple points along their course to the optic nerve, leading to lower thresholds. This is in contrast to column stimulation, where axons would only be stimulated at single points.

Finally, from a prosthesis engineering point of view, although both sequential stimulation of electrodes and simultaneous multiple-electrode stimulation may lead to similar interactions within the visual pathway, it will be much easier to implement the latter technique. Coupled with much lower electrode voltages and less charge required per electrode, stimulator designs, at least those based on providing constant current, would not require high compliance voltages. Also, data bandwidths and restrictions on stimulation rates would be reduced since multiple electrodes would be covered with a single stimulus. Having more time to stimulate the array would then possibly allow percepts to stay present and not fade, as presently seen with epiretinal and subretinal stimulation in blind humans (Perez Fornos A, et al. *IOVS* 2010;51:ARVO E-Abstract 3057).[3] We thus propose that ganged stimulation in the form of a line may be implemented to efficiently represent lines and edges of objects within a given image frame captured by the camera or, alternatively, groups of contiguous electrodes ganged together can be used to represent iso-brightness points in an image. These lines and groups of contiguous electrodes could themselves be sequentially presented, thus covering the entire retinal electrode array with representation of the whole image in a given scene. It of course remains to be seen whether ganged stimulation with a suprachoroidal electrode array would result in similar and reproducible percepts as those that have been reported in blind humans with epiretinal and subretinal arrays.[2,4,14] Determining this would be important as, despite the benefits seen with line stimulation and some evidence of retinotopically appropriate and localized cortical activation, the experiments performed in this study could not confirm if stimulation of a geometric line of electrodes would produce the perception of a line. While it would seem logical that stimulation of a geometric line would produce a perceptual line, ultimately this would depend on the various stages of retinal and cortical processing that would take place in order to determine the final percept. Nevertheless, as improved technology enables array fabrication with higher densities of electrodes with better charge-carrying capacities, the biggest challenge will always be to make efficient use of primitive phosphene percepts to provide meaningful and useful vision to the blind.

Acknowledgments

The authors thank Alexia Freemantle, Michelle McPhedran, and Elisa Borg for providing animal handling, assistance in surgery, and postoperative monitoring; Sue Pierce for veterinary advice; and Sam John, Joel Villalobos, and Tom Landry for their assistance in data collection.

References

1. de Balthasar C, Patel S, Roy A, et al. Factors affecting perceptual thresholds in epiretinal prostheses. *Invest Ophthalmol Vis Sci*. 2008;49:2303–2314.
2. Wilke R, Gabel VP, Sachs H, et al. Spatial resolution and perception of patterns mediated by a subretinal 16-electrode array in patients blinded by hereditary retinal dystrophies. *Invest Ophthalmol Vis Sci*. 2011;52:5995–6003.
3. Zrenner E, Bartz-Schmidt KU, Benav H, et al. Subretinal electronic chips allow blind patients to read letters and combine them to words. *Proc Biol Sci*. 2011;278:1489–1497.
4. Klauke S, Goertz M, Rein S, et al. Stimulation with a wireless intraocular epiretinal implant elicits visual percepts in blind humans: results from stimulation tests during the epiret3 prospective clinical trial. *Invest Ophthalmol Vis Sci*. 2011;52:449–455.
5. Fujikado T, Kamei M, Sakaguchi H, et al. Testing of semichronically implanted retinal prosthesis by suprachoroidal-transretinal stimulation in patients with retinitis pigmentosa. *Invest Ophthalmol Vis Sci*. 2011;52:4726–4733.
6. Hornig R, Zehnder T, Velikay-Parel M, Laube T, Feucht M, Richard G. The IMI retinal implant system. In: Humayun MS, Weiland JD, Chader G, Greenbaum E, eds. *Artificial Sight: Basic Research, Biomedical Engineering, and Clinical Advances*. New York: Springer-Verlag; 2007:111–128.
7. Rizzo JF III, Wyatt J, Loewenstein J, Kelly S, Shire D. Perceptual efficacy of electrical stimulation of human retina with a microelectrode array during short-term surgical trials. *Invest Ophthalmol Vis Sci*. 2003;44:5362–5369.
8. Rizzo JF III, Wyatt J, Loewenstein J, Kelly S, Shire D. Methods and perceptual thresholds for short-term electrical stimulation of human retina with microelectrode arrays. *Invest Ophthalmol Vis Sci*. 2003;44:5355–5361.
9. Keserü M, Feucht M, Bornfeld N, et al. Acute electrical stimulation of the human retina with an epiretinal electrode array. *Acta Ophthalmol*. 2012;90:e1–8. doi:10.1111/j.1755-3768.2011.02288.x.
10. Rizzo JF III. Update on retinal prosthetic research: the Boston retinal implant project. *J Neuroophthalmol*. 2011;31:160–168.
11. Guenther T, Lovell NH, Suaning GJ. Bionic vision: system architectures—a review. *Expert Rev Med Devices*. 2012;9:33–48.
12. Weiland JD, Cho AK, Humayun MS. Retinal prostheses: current clinical results and future needs. *Ophthalmology*. 2011;118:2227–2237.
13. Ong JM, Cruz LD. The bionic eye: a review. *Clin Experiment Ophthalmol*. 2012;40:6–17.
14. Humayun MS, de Juan E Jr, Weiland JD, et al. Pattern electrical stimulation of the human retina. *Vis Res*. 1999;39:2569–2576.
15. Black RC, Clark GM, Patrick JF. Current distribution measurements within the human cochlea. *IEEE Trans Biomed Eng*. 1981;28:721–725.
16. Shannon RV. Multichannel electrical stimulation of the auditory nerve in man. II. Channel interaction. *Hear Res*. 1983;12:1–16.
17. Townshend B, White RL. Reduction of electrical interaction in auditory prostheses. *IEEE Trans Biomed Eng*. 1987;34:891–897.
18. Seligman PM, Shepherd RK. Cochlear implants. In: Horch KW, Dhillon GS, eds. *Neuroprosthetics: Theory and Practice*. Singapore: World Scientific Publishing; 2004:878–904.
19. Wilke RG, Moghadam GK, Lovell NH, Suaning GJ, Dokos S. Electric crosstalk impairs spatial resolution of multi-electrode arrays in retinal implants. *J Neural Eng*. 2011;8:046016.
20. Dommel NB, Wong YT, Lehmann T, Dodds CW, Lovell NH, Suaning GJ. A CMOS retinal neurostimulator capable of focussed, simultaneous stimulation. *J Neural Eng*. 2009;6:035006.
21. Caspi A, Dorn JD, McClure KH, Humayun MS, Greenberg RJ, McMahon MJ. Feasibility study of a retinal prosthesis: spatial vision with a 16-electrode implant. *Arch Ophthalmol*. 2009;127:398–401.
22. Horsager A, Greenberg RJ, Fine I. Spatiotemporal interactions in retinal prosthesis subjects. *Invest Ophthalmol Vis Sci*. 2010;51:1223–1233.
23. Brindley GS, Lewin WS. The sensations produced by electrical stimulation of the visual cortex. *J Physiol*. 1968;196:479–493.
24. Shivdasani MN, Luu CD, Cicione R, et al. Evaluation of stimulus parameters and electrode geometry for an effective suprachoroidal retinal prosthesis. *J Neural Eng*. 2010;7:036008.
25. Villalobos J, Allen PJ, McCombe MF, et al. Development of a surgical approach for a wide-view suprachoroidal retinal

prosthesis: evaluation of implantation trauma. *Graefes Arch Clin Exp Ophthalmol*. 2012;250:399–407.

26. John SE, Shivdasani MN, Leuenberger J, et al. An automated system for rapid evaluation of high-density electrode arrays in neural prostheses. *J Neural Eng*. 2011;8:036011.
27. Tusa RJ, Palmer LA, Rosenquist AC. The retinotopic organization of area 17 (striate cortex) in the cat. *J Comp Neurol*. 1978;177:213–235.
28. Heffer LF, Fallon JB. A novel stimulus artifact removal technique for high-rate electrical stimulation. *J Neurosci Methods*. 2008;170:277–284.
29. Wilson JR, Sherman SM. Receptive-field characteristics of neurons in cat striate cortex: changes with visual field eccentricity. *J Neurophysiol*. 1976;39:512–533.
30. Hubel DH, Wiesel TN. Receptive fields of single neurones in the cat's striate cortex. *J Physiol*. 1959;148:574–591.
31. Eckhorn R, Wilms M, Schanze T, et al. Visual resolution with retinal implants estimated from recordings in cat visual cortex. *Vis Res*. 2006;46:2675–2690.
32. Elfar SD, Cottaris NP, Iezzi R, Abrams GW. A cortical (V1) neurophysiological recording model for assessing the efficacy of retinal visual prostheses. *J Neurosci Methods*. 2009;180:195–207.
33. Loizou PC. Mimicking the human ear. *Signal Processing Magazine, IEEE*. 1998;15:101–130.
34. Horsager A, Boynton GM, Greenberg RJ, Fine I. Temporal interactions during paired-electrode stimulation in two retinal prosthesis subjects. *Invest Ophthalmol Vis Sci*. 2011;52:549–557.
35. Martinez LM, Alonso JM. Construction of complex receptive fields in cat primary visual cortex. *Neuron*. 2001;32:515–525.
36. Hubel DH, Wiesel TN. Receptive fields, binocular interaction and functional architecture in the cat's visual cortex. *J Physiol*. 1962;160:106–154.
37. Leventhal AG, Schall JD. Structural basis of orientation sensitivity of cat retinal ganglion cells. *J Comp Neurol*. 1983;220:465–475.
38. Levick WR, Thibos LN. Analysis of orientation bias in cat retina. *J Physiol*. 1982;329:243–261.